UNIVERSITY OF MISKOLC

Faculty of Mechanical Engineering and Information Technology

DEVELOPMENT AND EVALUATION OF THERMAL MODELS FOR ANGULAR CONTACT BALL BEARINGS IN SPINDLE SYSTEMS

PhD Dissertation

Author:

Sebastián Cabezas
Mechatronics Engineering (BSc),
Mechanical Engineering (MSc)

István Sályi Doctoral School of Mechanical Engineering Sciences

Head of Doctoral School
Dr. Gabriella Bognár
DSc Full Professor

Head of Topic Group
Dr. György Hegedűs
Associate Professor

Scientific Supervisors
Dr. György Hegedűs
Associate Professor
Dr. Péter Bencs
Associate Professor

Miskolc, 2025

Judging Committee

Chair:

Secretary:

Member:

Official Reviewers

1 Introduction and Objectives

A crucial factor influencing precision and accuracy in machine tools is the thermal behavior of the spindle units. Thermal errors in spindle units account for 60-70 % of the total errors of machine-tools, leading to critical conditions including permanent deformation of the machine elements, low machining precision, material wear, reduction of service life span, internal heat generation and dissipation, improper dynamic behavior, among other concerns. Recent investigations demonstrate that the rolling bearings of the spindle units are highly impacted by the temperature increase within the spindle unit, which determine the structural temperature fluctuation in machining processes. Angular contact ball bearings are mainly used in spindle units due to their capacity to accommodate and distribute radial and thrust loads produced due to external machining operations. Furthermore, this type of bearing is suitable for implementation in spindles due its proper performance at high rotational speeds maintaining shaft balance. However, not only the forces acting on the bearings and the rotational speed determine the thermal behavior of these elements. It is also necessary to analyze and investigate essential factors including the assembly geometry and bearing arrangement, the effects of internal lubrication in the bearing, and stress analysis in the contact area between the inner components of the bearing (inner-ring, balls, outer-ring), and the combinations of thermal contact resistances.
The present PhD dissertation has as primary objective the development of new thermal models to determine the temperature distribution in rolling bearings, specifically angular contact ball bearings of spindle systems based on the global identification of low order lumped parameter thermal networks.

1.1 Objectives

The investigation, design and development of the thermal networks in this work has the following specific objectives:

- Conducting an extensive research based on recent and previous investigations related to the methodologies and theories of thermal analysis in rolling bearings, aiming to establish advancements made in this field. Subsequently, establish the current state of the art, which mainly focuses on thermal models for angular contact ball bearings of spindle units.
- Developing three thermal networks for angular contact ball bearings based on the global identification of low-order lumped parameter thermal networks and the heat transfer theory. The models involve the analysis of bearing configurations, the forces acting during machining operations, the

analysis of frictional moments due to the contact between the inner components of the bearing, the lubrication type and its influence on heat dissipation, the generation of heat and the its main contributors.

- Implementing thermal resistances for real contact heat sources of stationary, moving and combined conditions, which arise due to elliptical contact. This implementation is based on the mathematical solutions proposed by Y. S. Muzychka and M.M. Yovanovich, along with the Hertzian contact theory. Furthermore, to enhance the predictability of the models, Mellor's formulation for cylindrical geometries for analyzing axial and radial heat flow is implemented on the inner- and outer-ring of the bearing.

- Setting up two methods of solution of the thermal models, which are mathematically represented by systems of first-order ordinary homogeneous differential equations. The first novel methodology, is based on the state space approach, solving the thermal models as Multiple Input, Multiple Output (MIMO) systems for both stationary and transient state. The second methodology is based on the solution of continuous time-dependent systems. Both, the state-space approach and the continuous time dependent systems are solved using Python.

- Testing and validating the thermal models using FEA solutions based on ANSYS steady and transient state thermal. The simulations will be performed considering the elements of the angular contact ball bearing as separate, independent entities, while utilizing heat generation analysis as initial and boundary conditions. Furthermore, the effects of lubrication are implemented and analyzed through convective heat transfer analysis.

- Testing and validating the new lumped parameter thermal models experimentally using a bearing testing rig. In this rig, a representative model consisting of an angular contact ball bearing model SFK 7203BEP placed inside a housing emulates a rolling bearing in a spindle unit. Controlled radial force and rotational speed, and measurements are taken using Type-J thermocouples placed on the surfaces of the static elements of the representative model, including the housing and the outer-ring of the bearing. Additionally, a thermal camera is used to obtain measurements of the rotational parts, including the surface of the inner-ring and the surface of the cross-section of the shaft.

2 Methodology of Study

The present chapter describes the methodology applied for the development of the thermal models: Dark Gray-Box, Light Gray-Box, and White Box Lumped parameter thermal networks (LPTN). All the necessary concepts for the creation of the thermal models including, type of bearing arrangement, external and internal parameters, the rolling contact analysis, the frictional model, the heat generation, the thermal contact resistances, and the methods of solution are extensively analized to develop the new lumped parameter thermal models.

The block diagram depicted in Fig. 2, shows the stages in a general overview for the development of the thermal models. To begin with, the type of bearing arrangement used in spindle units is presented. The same arrangement is implemented in the representative model for the validation of the thermal models. Following that, the external and internal factors influencing the thermal behavior are described. These factors include external loads, lubrication type, and operational speeds. Then, the rolling contact analysis must be performed based on the Hertzian contact theory for elliptic contact. The external and internal parameters along with the rolling contact analysis are foundation for the determination of the sliding frictional moment M_{sl} and rolling friction M_{rr}, which determine the total frictional moment M_f. Following this analysis, the heat generation is calculated. The heat partition concept is implemented to determine the heat generation in the outer-ring $\dot{Q}_o$, the balls $\dot{Q}_b$, and the inner-ring $\dot{Q}_i$, of the bearing; and the heat distribution is analyzed based on the heat transfer laws. The thermal contact resistances for static, moving and combined heat sources, along with the axial and radial flow analysis are determined in the following stage. Finally, these factors, along with the heat generation and the thermal characteristics of the rolling bearing components, are implemented in the new lumped parameter thermal models. For solving the system of differential equations, the new proposal based on the state-space approach is given, calculating the heat distribution in steady and transient state. Euler's method is implemented to determine the continuous time dependent function of the thermal models. The final stage is the verification of the thermal models.

2.1 Representative model of the bearing arrangement

A representative model, which embodies the bearing arrangement in a spindle unit, is depicted in Fig. 2a. The angular contact ball bearings are used in spindle units due to their capacity to accommodate radial and axial loads at high rotational speeds. Further advantages of implementing the back-to-back arrangement include the capacity to resist highest moment its ability to handle tilting loads. When

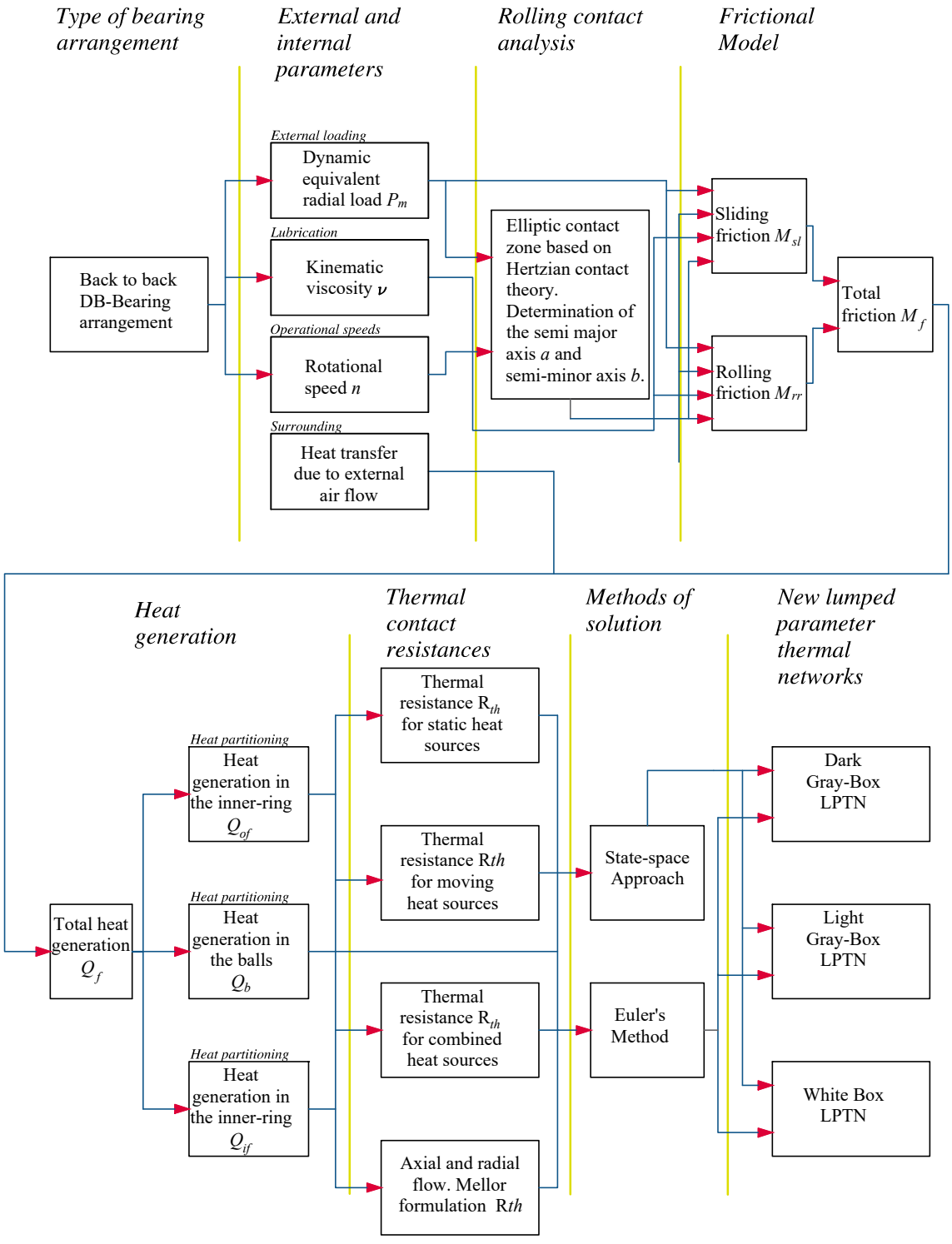

Figure 1: Block diagram of the thermal analysis of rolling bearings in spindle units

the temperature increases, the radial expansion will tend to increase the pre-load of the bearings. To mitigate this effect, the axial growth allows the bearings to move. Therefore, this type of arrangement is implemented in high-temperature / high-speed applications. The representative model selected in this study consists of two angular contact ball bearings, model SKF 7203BEP, mounted on a shaft with bore diameter equal to that of the bearings. The bearings are packed on a housing, which, for the

experimental analysis will be loaded in the radial direction under rotational speed, emulating the basic equivalent radial load P_m produced during machining operations.

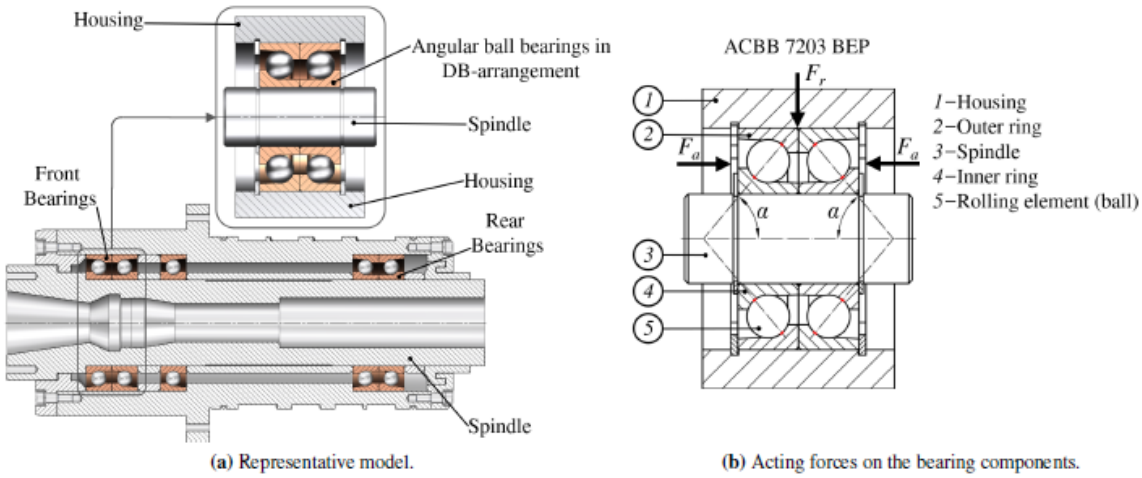

(a) Representative model. (b) Acting forces on the bearing components.

Figure 2: Bearing arrangement in a spindle unit

2.2 Dynamic equivalent radial load

During machining operations, forces are exerted by the contact between the machine tool and the workpiece. These forces are primarily absorbed by the angular contact ball bearings and are classified as axial F_a and radial loads F_r [34] (see Fig. 2b). The magnitude of these loads varies according to the contact angle α. The combination of axial F_a and radial F_r loads is referred to as the dynamic equivalent radial load P_m [30], as given in Eq. (1).

$$\begin{aligned} \frac{F_a}{F_r} &\leq 0.505 \cdot \left(\frac{F_a}{C}\right)^{0.231} \quad ; \quad P_m = F_r \\ \frac{F_a}{F_r} &> 0.505 \cdot \left(\frac{F_a}{C}\right)^{0.231} \quad ; \quad P_m = 0.56 \cdot F_r + \frac{0.84 \cdot F_a}{\left(\frac{F_a}{C}\right)^{0.24}} \end{aligned} \tag{1}$$

2.3 Determination of the rolling contact

According to Hertzian classic theory, when two elastic bodies (inner-ring and ball, or outer-ring and ball) are subjected to pressure generated by external forces, the contact area has the shape of an ellipse of semi-major axis a and semi-minor axis b, given in Eq. (2).

$$\begin{aligned} a_{IR,OR} &= \xi \left[\frac{3P_m}{\left(\frac{1-\upsilon^2}{E}\right)\sum \rho_{IR;OR}}\right]^{1/3} ; \\ b_{IR,OR} &= \eta \left[\frac{3P_m}{\left(\frac{1-\upsilon^2}{E}\right)\sum \rho_{IR;OR}}\right]^{1/3} \end{aligned} \tag{2}$$

2.3.1 Determination of the kinematic viscosity

The Vogel and Walther approaches for the determination of the kinematic viscosity ν are determined by Eq. (3) and Eq. (4), respectively.

$$\nu = \nu_{ref} \cdot \exp\left(-\beta\left(T_{lub} - T_{lref}\right)\right), \tag{3}$$

where $\beta = \frac{\ln \frac{\nu_{lf}}{\nu_{li}}}{T_{li} - T_{lf}}$, depends on the kinematic viscosity of the lubricant at ambient temperatures and a maximum value of temperature T_{lf} that for this analysis is 150°C.

$$\nu = \log\log\left(\nu_{lf} + 0.7\right) - \frac{\log\log\left(\nu_{lf} + 0.7\right) - \log\log\left(\nu_{li} + 0.7\right)}{\log\left(\frac{T_{lf}}{T_{li}}\right)} \cdot \log\left(T_{lf}\right) \tag{4}$$

2.3.2 Determination of the fluid film thickness

A minimum lubricant film thickness must be formed in order to support the loads and allow the rotating movement of the balls and rings of the bearing. The film thickness given in Eq. (5) is determined as a function of three main coefficients, the dimensionless speed parameter U^*, the dimension load parameter W^* and the dimensionless material parameter G^*.

$$H_{IR,OR} = 3.63 \cdot U_{IR,OR}^{*0.68} \cdot W_{IR,OR}^{*-0.073} \cdot G^{*0.49} \cdot \left[1 - \exp\left(-0.68 \cdot 1.03 \frac{b_{IR,OR}}{a_{IR,OR}}\right)\right] \tag{5}$$

2.3.3 Determination of the convective coefficient of the lubricant film

Heat transfer by convection occurs between the oil-film and the inner-ring, the oil-film and the balls, the oil-film and the outer ring. The heat convection coefficient of the lubricant were obtained as functions of the Nusselt number Nu, and are given in Eq. (6).

$$h_i = \frac{k_{oil} \cdot Nu_i}{d_2}, \quad h_b = \frac{k_{oil} \cdot Nu_b}{D_w}, \quad h_o = \frac{k_{oil} \cdot Nu_o}{D_1} \tag{6}$$

2.4 Convective coefficients of air surrounding the housing

The surroundings of a spindle system play an important role in heat transfer analysis. Mainly, spindles are exposed to ambient air that flows at very low speeds.Through convection, the air dissipates heat transferred from the housing. The heat convection coefficient of the surroundings was calculated using Eq. (7)

$$h_{air} = Nu_{air} \cdot \frac{k_{air}}{\phi_{housing}} \tag{7}$$

2.5 Determination of the frictional moments

Based on Palgrem's empirical model, the frictional moments can be calculated. It has been discussed in the previous sections that the present investigation considers the rolling friction M_{rr} and sliding friction M_{sl} for the determination of the total frictional moment M_f . For the representative model an ACBB 7203BEP is used as sample; therefore, it can be possible to use the own formulation proposed for the determination of frictional moments. The mathematical formulation is given in Eq. (8).

$$
\begin{aligned}
M_{sl} &= 1.82 \cdot 10^{-12} \cdot d_m^{0.26} \cdot \left[\left(F_r + 2.44 \cdot 10^{-12} \cdot d_m^4 \cdot n^2 \right)^{\frac{4}{3}} + 0.71 \cdot F_a^{\frac{4}{3}} \right] \cdot \mu_{sl} \\
M_{rr} &= \Phi_{isl} \cdot \Phi_{rs} \cdot 4.33 \cdot 10^{-7} \cdot d_m^{1.97} \cdot \left(F_r + 2.44 \cdot 10^{-12} \cdot d_m^4 \cdot n^2 + 2.02 \cdot F_a \right)^{0.54} \cdot (\nu \cdot n)^{0.6} \\
M_f &= M_{sl} + M_{rr}
\end{aligned}
\tag{8}
$$

2.6 Determination of the heat generation

Based on previous investigations, it is understood that the components are not in thermal equilibrium, and the heat generation is not constant. Therefore, heat must be distributed accordingly. The heat partitioning theory was established in this work. The inner-ring is considered to absorb 25 % of the total heat generation, as in the outer-ring. The balls are considered to absorb 50 % of the total heat generated. The total heat generation was determined as a function of the total frictional moment M_f and is given in Eq. (9).

$$
\begin{aligned}
\dot{Q}_f &= \frac{2 \cdot \pi \cdot n}{60} \cdot 10^{-3} \cdot M_f \\
\dot{Q}_b &= 0.50 \cdot \dot{Q}_f, \; \dot{Q}_i = 0.25 \cdot \dot{Q}_f, \; \dot{Q}_o = 0.25 \cdot \dot{Q}_f
\end{aligned}
\tag{9}
$$

2.7 Thermal contact resistances

The intention of modeling the components of the angular contact ball bearing in the spindle unit as a thermal network, depends on the correct conceptualization of the thermal resistances and the appropriate selection of the nodes that compound the thermal network. The angular contact ball bearing will be modeled as a control volume that can be subdivided into finite sub-volumes (nodes). The effectiveness of the thermal network will depend on the capacity of each node to carry information, such as temperature T, and heat generation Q. This can be achieved if the connections of the nodes (thermal resistances), are sufficient to describe the heat transfer phenomena accurately.

In this section, the general formulations utilized for the determination of the thermal resistances are tabulated in Table 1. This formulations are later implemented in each of the the three thermal models that are proposed in this PhD dissertation.

Table 1: Thermal resistances of the Dark Gray-Box LPTN

Denomination	Formulation	Type
Cylindrical geometry	$R_{th} = \frac{\ln\left(\frac{r_{ext}}{r_{int}}\right)}{2\pi \cdot k \cdot L}$	Conduction
Mellor Formulation	$Ra_{th,IR;OR} = \frac{L}{6\pi k\left(r_{ext.}^2 - r_{int.}^2\right)}$ $Rb_{th,IR;OR} = \frac{1}{2\pi kL}\left[1 - \frac{2r_{int.}^2 \ln\left(\frac{r_{ext.}}{r_{int.}}\right)}{\left(r_{ext.}^2 - r_{int.}^2\right)}\right]$ $Rc_{th,IR;OR} = \frac{1}{2\pi kL}\left[\frac{2r_{ext.}^2 \ln\left(\frac{r_{ext.}}{r_{int.}}\right)}{\left(r_{ext.}^2 - r_{int.}^2\right)} - 1\right],$ $Rm_{th,IR;OR} = \frac{-1}{4\pi kL\left(r_{ext.}^2 - r_{int.}^2\right)}\left[r_{ext.}^2 + r_{int.}^2 - \frac{4r_{ext.}^2 r_{int.}^2 \ln\frac{r_{ext.}}{r_{int.}}}{\left(r_{ext.}^2 - r_{int.}^2\right)}\right]$	Conduction
Stationary	$\overline{Rs}_{th} = \frac{16}{3\pi^3 k\sqrt{A_{OR}}} \cdot \sqrt{\pi\epsilon_s} K_1\left(\epsilon_s^{'}\right)$ $\hat{Rs}_{th} = \frac{2}{\pi^2 k\sqrt{A_{OR}}} \cdot \sqrt{\pi\epsilon_s} K_1\left(\epsilon_s^{'}\right)$	Conduction
Moving	$\overline{Rmo}_{th} = \frac{0.750}{k\sqrt{A_{IR;OR}} Pe^*_{\sqrt{A_{IR;OR}}}}$ $\hat{Rmo}_{th} = \frac{1.20}{k\sqrt{A_{IR;OR}} Pe^*_{\sqrt{A_{IR;OR}}}}$	Conduction
Combined	$\overline{Rco}_{th} = \frac{0.750}{k\sqrt{A_{IR;OR}}\left(Pe^*_{\sqrt{A_{IR;OR}}} + \frac{6.05}{\epsilon_s K_1^2\left(\epsilon_s^{'}\right)}\right)}$ $\hat{Rco}_{th} = \frac{1.20}{k\sqrt{A_{IR;OR}}\left(Pe^*_{\sqrt{A_{IR;OR}}} + \frac{11.16}{\epsilon_s K_1^2\left(\epsilon_s^{'}\right)}\right)}$	Conduction
Constriction	$Rcons_{th} = \frac{F_{Roess}}{4 \cdot l_a \cdot k}$	Constriction
Convection	$R_{th,h} = \frac{1}{A_h \cdot h_{air}}$ $R_{th,or} = \frac{1}{A_o \cdot h_o}$ $R_{th,b} = \frac{1}{A_b \cdot h_b}$ $R_{th,ir} = \frac{1}{A_i \cdot h_i}$	Convection

2.8 State Space Method for monitoring thermal fields in rolling bearings of spindle systems

This methodology has wide applications in control systems with two primary focuses: control and monitoring. Due to its advantages, including the analysis of multi-variable systems, non-linear and time variant systems, and the capabilities of monitoring design approaches, I have considered this technique applicable for the determination of the thermal fields in my research.

In the angular contact ball bearing, I have set a number of variables that define the thermal system of the rolling bearing, these are the thermal fields analized for each of the three thermal models (Dark Gray-Box, Light Gray-Box, and White Box LPTN), which will be described at detail in the results. The input variables were simplified to the environmental temperatures and the heat generation $\dot{Q}$.

The state equation is defined as a matrix function of the state vector differential equation, and is given in Eq. (10).

$$\begin{aligned} \dot{x} &= Ax + Bu \\ y &= Cx + Du \end{aligned} \tag{10}$$

3 Dark Gray-Box LPTN

The Dark Gray-Box LPTN was conceived as a low order thermal network consisting of five nodes, which are necessary to describe the thermal fields of the housing and outer-ring T_{ho}, the balls T_b, and the inner-ring T_i. The housing and the outer-ring were established as a unique body, considering that these two elements are static and possess equivalent thermal properties, including thermal conductivity k and specific heat c_p. Similar consideration was established for the inner-ring and shaft, which are coupled components rotating at equal movement. The thermal nodes are: N_1, which represents the surroundings of the housing; N_2, which represents the housing and outer-ring; N_3, which represents the lubricant film; N_4, which represents the ball; and N_5, which represents the inner-ring and shaft.

The system of equations presented in Eq. (11) represents the new low order lumped parameter thermal network.

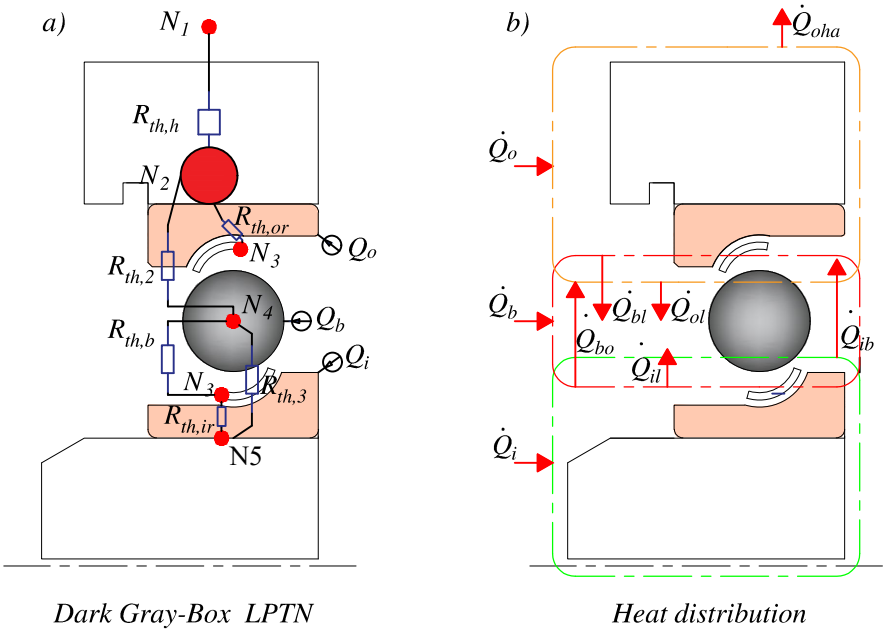

Figure 3: a) Dark Gray-Box LPTN. b) Energy distribution through the bearing

$$
\begin{aligned}
m_{oh}c_p\frac{dT_{oh}}{dt} &= \dot{Q}_o - T_{oh}\left(\frac{1}{R_{th,2}}+\frac{1}{R_{th,or}}+\frac{1}{R_{th,h}}\right)+\frac{T_b}{R_{th,2}}+\frac{T_{N_3}}{R_{th,or}}\\
Nm_bc_p\frac{dT_b}{dt} &= \dot{Q}_b + \frac{T_{oh}}{R_{th,2}} - T_b\left(\frac{1}{R_{th,2}}+\frac{1}{R_{th,b}}+\frac{1}{R_{th,3}}\right)+\frac{T_i}{R_{th,3}}+\frac{T_{N_3}}{R_{th,ir}}\\
m_ic_p\frac{dT_i}{dt} &= \dot{Q}_i + \frac{T_b}{R_{th,3}} - T_i\left(\frac{1}{R_{th,3}}+\frac{1}{R_{th,ir}}\right)+\frac{T_{N_3}}{R_{th,ir}}
\end{aligned}
\tag{11}
$$

3.1 Solutions in stationary state using the State-Space approach

The mathematical model was developed as an observer, meaning that the model has the capacity to predict the thermal behavior of the system. To achieve this, the State-Space approach is applied. The system is considered as a multiple-input and multiple-output system, in which the state variables are determined as a step response of a first order dynamic system (T_{oh}, T_b, T_i). The inputs of the system are the rotational speed, the external forces, and the frictional moments. However, this variables are represented in the system as the heat generation $\dot{Q}$, the inner temperature of the lubricant T_{N_3} in Eq. (11), and the heat by convection from the surroundings expressed by the temperature T_{air}. The final system equation of the Dark Gray-Box LPTN, expressed in state-space response is given in Eq. (12).

$$
\begin{bmatrix} m_{oh}c_pT_{oh}^{\cdot} \\ Nm_bc_p\dot{T_b} \\ m_ic_p\dot{T_i} \end{bmatrix} = \begin{bmatrix} -\left(\frac{1}{R_{th,2}}+\frac{1}{R_{th,or}}+\frac{1}{R_{th,h}}\right) & \frac{1}{R_{th,2}} & 0 \\ \frac{1}{R_{th,2}} & -\left(\frac{1}{R_{th,2}}+\frac{1}{R_{th,or}}+\frac{1}{R_{th,h}}\right) & \frac{1}{R_{th,3}} \\ 0 & \frac{1}{R_{th,3}} & -\left(\frac{1}{R_{th,3}}+\frac{1}{R_{th,ir}}\right) \end{bmatrix} \begin{bmatrix} T_{oh} \\ T_b \\ T_i \end{bmatrix} + \begin{bmatrix} 0.25 & \frac{1}{R_{th,h}} & \frac{1}{R_{th,or}} \\ 0.5 & 0 & \frac{1}{R_{th,ir}} \\ 0.25 & 0 & \frac{1}{R_{th,ir}} \end{bmatrix} \begin{bmatrix} \dot{Q} \\ T_{air} \\ T_{N_3} \end{bmatrix}
$$

$$
y = \begin{bmatrix} 1 & 0 & 0 \\ 0 & 1 & 0 \\ 0 & 0 & 1 \end{bmatrix} \begin{bmatrix} T_{oh} \\ T_b \\ T_i \end{bmatrix} \tag{12}
$$

To validate the solution of the system under steady-state conditions, FEA simulations were performed, along with experimental measurements. The experimental measurements were carried out using an experimental rig on which the representative model was mounted. The forces were exerted by a hydraulic piston emulating the dynamic equivalent radial load P_m , which was measured using a force transducer, and the rotational speed was changed using a variable frequency driver. Thermocouples type J were conected to the static parts of the system, these are: the outer-ring and the housing.

Experiment 1)

In this experiment, the maximum value of $P_m = 5.66$ kN, allowed by the bearing manufacturer, and the maximum value of rotational speed $n = 2890$ rpm that can be achieved in the experimental testing jig, were established. The main objective of this experimental analysis was to determine the thermal fields under limit conditions. Steady state conditions were reached at $t = 150$ s. It is evident that the temperature increase under these conditions is excessive, as depicted in Fig. (4). However, the model

can predict the temperature behavior accordingly.

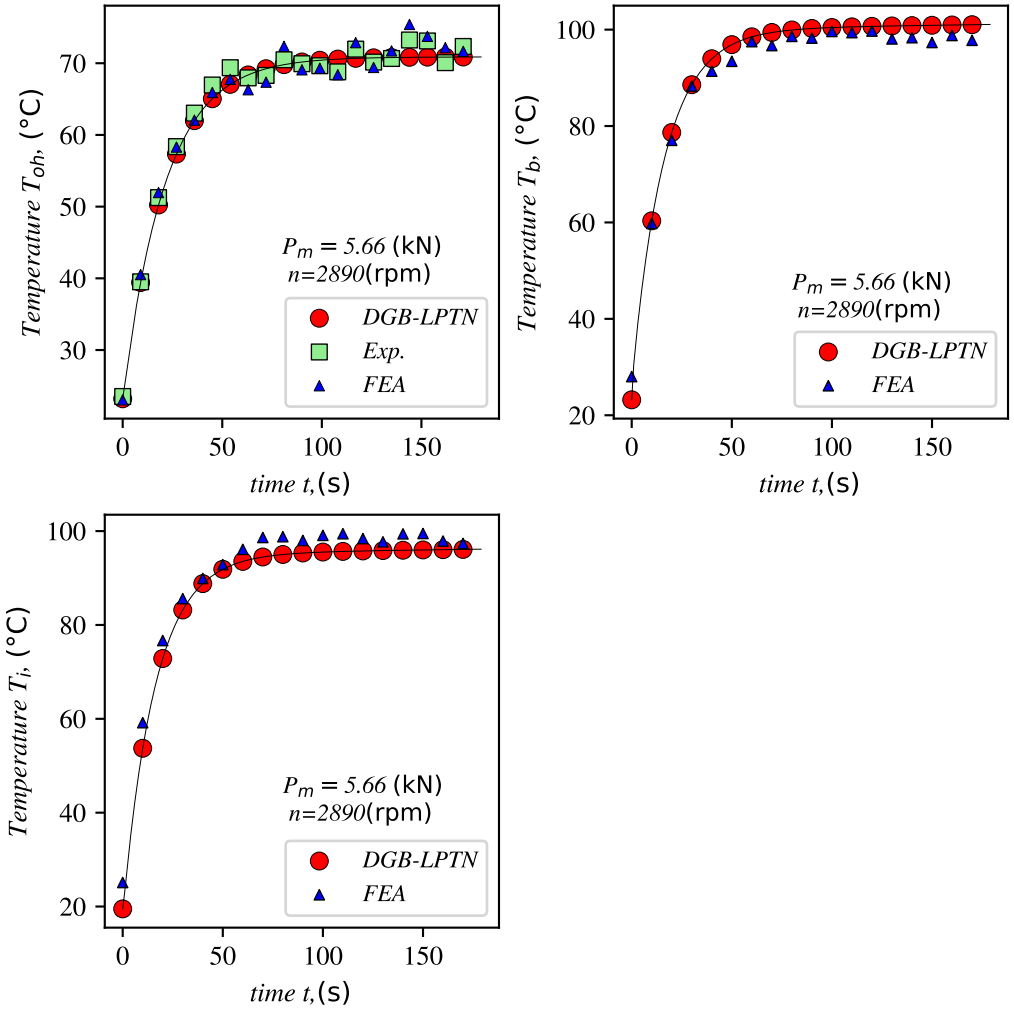

Figure 4: Dark Gray-Box LPTN $P_m = 5.66$ kN, $n = 2890$ rpm.

3.2 Solutions in continuous time

Experiment 2)

In this experiment, the rotational speed was set to an average working speed in the test jig, $n = 1300$ rpm, the force P_m follows the same pattern as in all the experiments per. The thermal behavior is shown in Fig. (5).

Many experiments were evaluated in the same way as depicted in Figures Fig. (5), using different values of rotational speed: $n = 500$ rpm, $n = 898$ rpm, $n = 1300$ rpm, $n = 1695$ rpm, $n = 2491$ rpm, and $n = 2890$ rpm. The tests were performed during the same time range, and the standard deviation was evaluated at each second s . The purpose of this statistical evaluation was to analyze the accuracy of the new model compared to experimental measurements and the FEA simulations. The dispersion results are illustrated in Fig. (6).

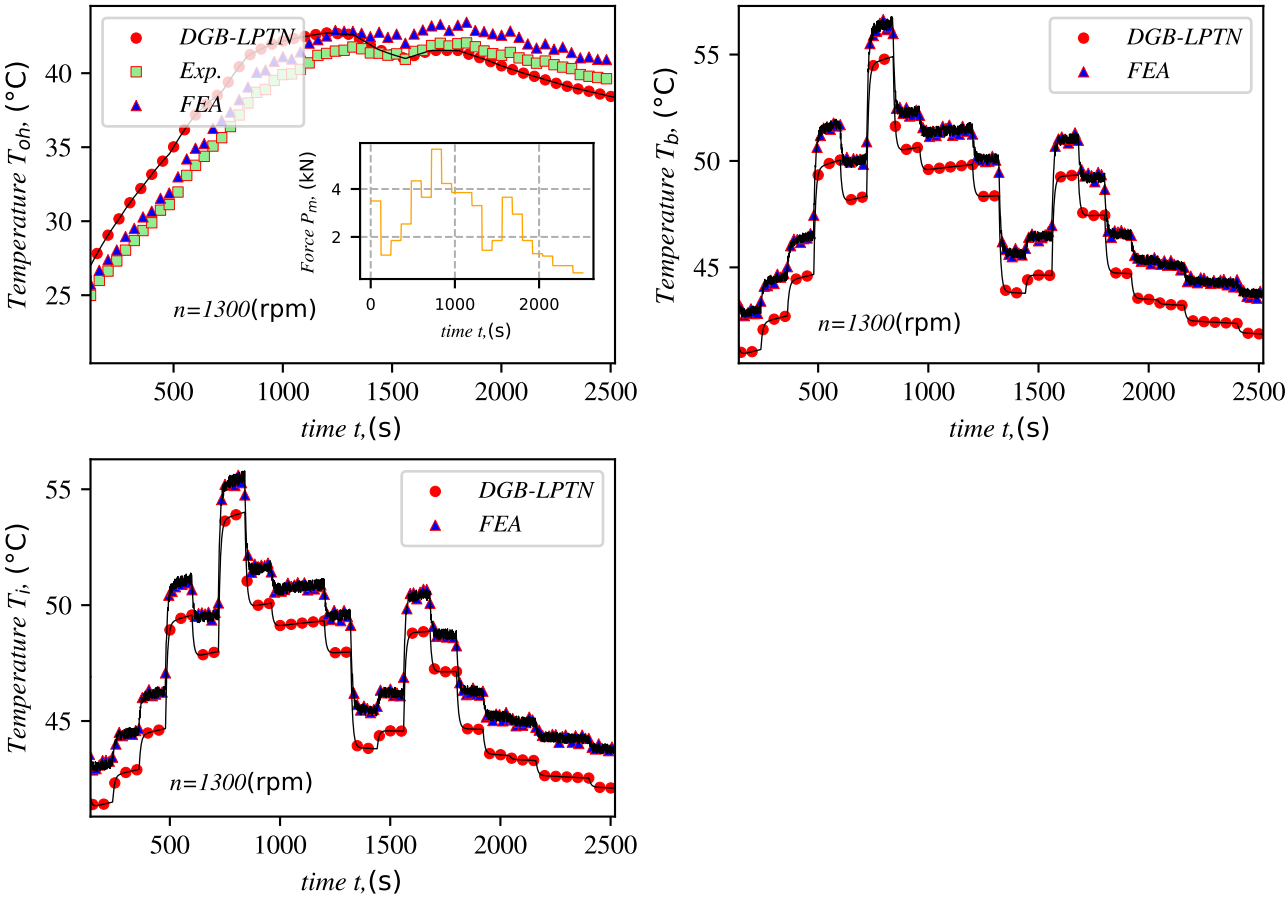

Figure 5: Dark Gray-Box LPTN. Continuous time solution $n = 1300$ rpm.

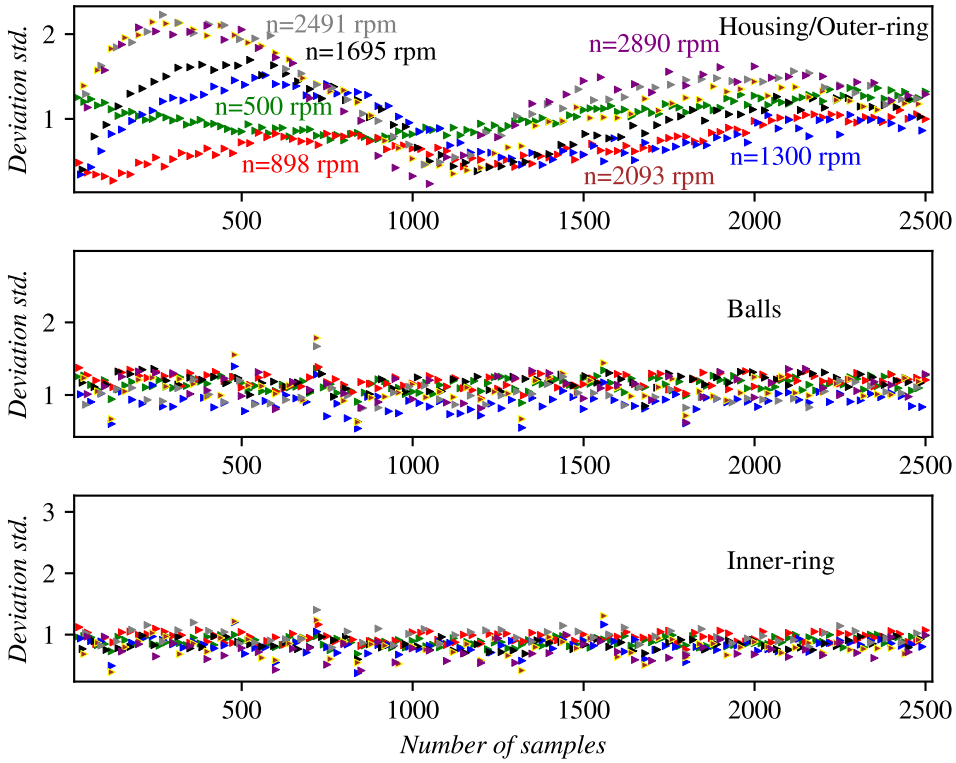

Figure 6: dispersion analysis for the components of the rolling bearing using the Dark Gray-Box LPTN model.

4 Light Gray-Box and White-Box LPTN

The Light Gray-Box LPTN, illustrated in Fig. (7), is a low-order thermal network (Low number of nodes), requiring low local discretization. However, the elements of the thermal network can be reliably divided to ensure the independent analysis of each element in the representative model. The thermal material properties, geometrical characteristics, contact between the surfaces of the elements, and the formulation of the heat transfer theory form the basis for creating this thermal network. Furthermore, it enables the application of moving heat sources for the analysis of the thermal contact resistances between the inner ring and the balls and the outer ring and the balls. The Light Gray-Box LPTN was conceived as follows: 9 diffusion nodes, 10 thermal resistances and 3 heat sources.
The White-Box LPTN, illustrated in Fig. (8), is a low order thermal network, with an accurate level of discretization. It enables the division of the inner elements into small nodes, hence enhancing the prediction of the thermal fields of the inner component of the bearing. This type of thermal network is built upon principles of heat transfer theory, the thermal properties of the materials, the geometrical constraints, thermal contact resistances for stationary, moving, and combined heat sources. Additionally, the thermal resistances of the inner ring, outer ring and shaft were determined by the Mellor formulation [94] to ensure a more precise prediction of the thermal fields. The White Box LPTN was conceived as follows: 17 diffusion nodes, 20 thermal resistances and 3 heat sources.

The mathematical model for the Light Gray-Box LPTN, and for the White-Box LPTN, are given in Eq. (13) and Eq. (14), respectively.

$$
\begin{aligned}
m_h c_p \frac{dT_h}{dt} &= \frac{T_o - T_h}{\frac{1}{\left(R_{th,1}+R_{th,2}\right)} + \frac{1}{R_{th,3}}} - \frac{T_h - T_a}{R_{th,h}} \\
m_o c_p \frac{dT_o}{dt} &= \dot{Q}_o - \frac{T_o - T_h}{\frac{1}{\left(R_{th,1}+R_{th,2}\right)} + \frac{1}{R_{th,3}}} - \frac{T_o - T_b}{R_{th,4}} - \frac{T_o - T_l}{R_{th,or}} \\
N m_b c_p \frac{dT_b}{dt} &= \dot{Q}_b + \frac{T_o - T_b}{R_{th,4}} - \frac{T_o - T_b}{R_{th,4}} - \frac{T_b - T_i}{R_{th,5}} - \frac{T_b - T_l}{R_{th,b}} \\
m_i c_p \frac{dT_i}{dt} &= \dot{Q}_i + \frac{T_b - T_i}{R_{th,5}} - \frac{T_i - T_s}{R_{th,6}} - \frac{T_i - T_l}{R_{th,ir}}
\end{aligned}
\tag{13}
$$

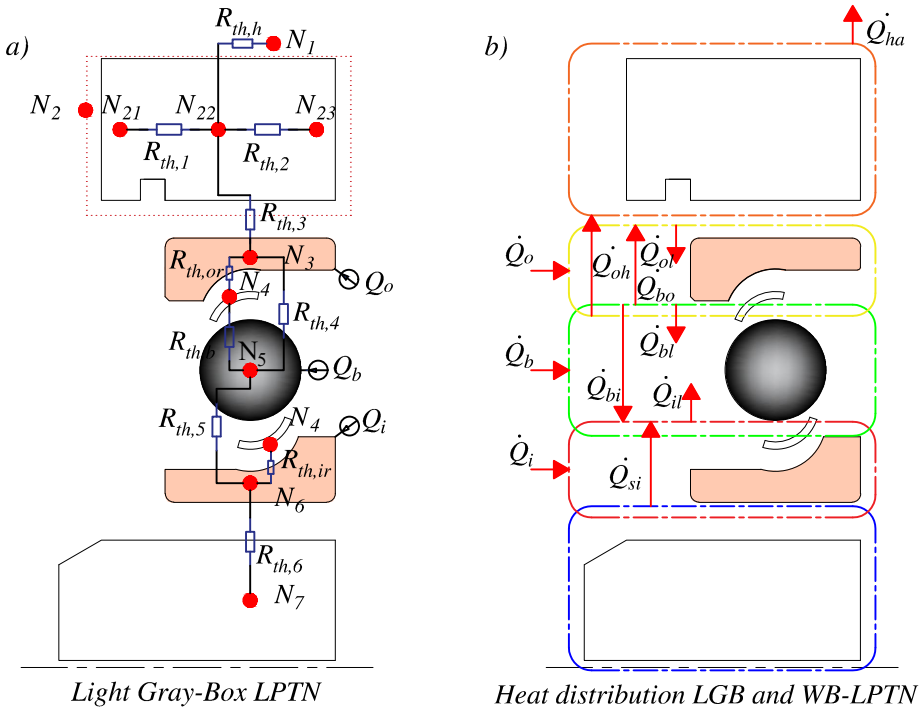

Figure 7: a) Light Gray-Box LPTN. b) Energy distribution through the bearing for the Light Gray-Box and White-Box LPTN.

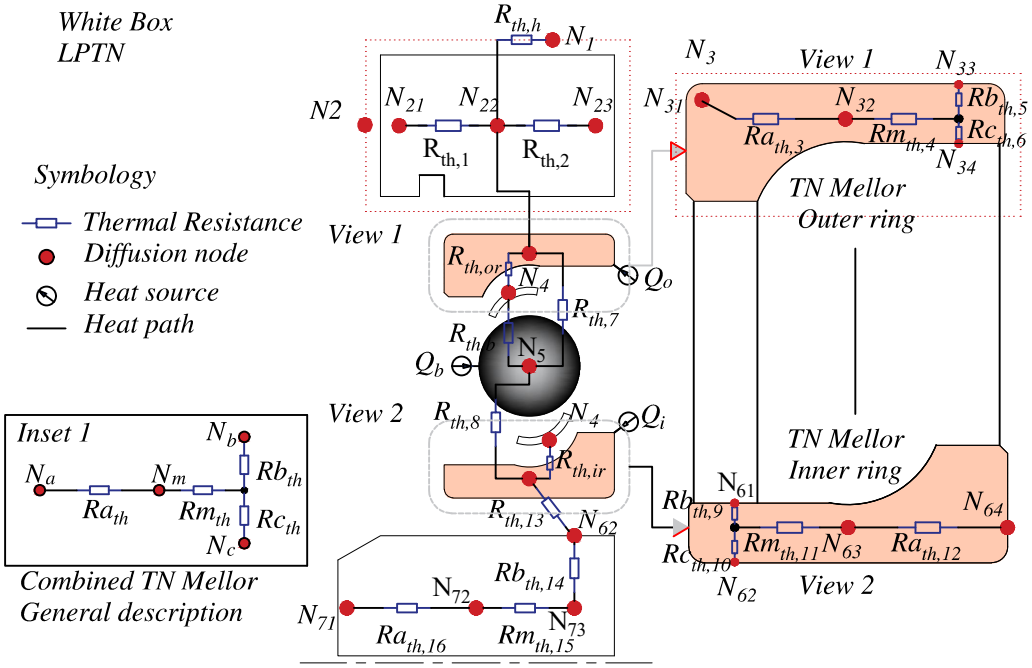

Figure 8: a) White-Box LPTN.

Statistical analysis was performed to show the dispersion of the thermal model in comparison to the FEA, and experimental measurements. In comparison to the Dark Gray-Box LPTN, and the Light Gray-Box LPTN, the White-Box LPTN shows more accurate results. For the housing T_h, the maximum dispersion was 0.67, the remaining values are within the range $0.21 - 0.68$. For the outer-ring T_o, the maximum dispersion was 1.33, the remaining values are within the range $0.29 - 1.33$. For the balls T_b,

the maximum dispersion was 1.04, the remaining values are within the range $0.0 - 1.04$. Finalle, for the inner-ring T_i, the maximum dispersion was 0.99, the remaining values are within the range $0.0 - 0.99$. The graphic of dispersion for the Light Gray-Box and White-Box LPTN are given in Fig. (9) and Fig. (10), respectively.

$$
\begin{aligned}
m_h c_p \frac{dT_h}{dt} &= \frac{T_o - T_h}{\frac{1}{\left(R_{th,1}+R_{th,2}\right)} + \frac{1}{R_{th,mellor(or)}}} - \frac{T_h - T_a}{R_{th,h}} \\
m_o c_p \frac{dT_o}{dt} &= \dot{Q}_o - \frac{T_o - T_h}{\frac{1}{\left(R_{th,1}+R_{th,2}\right)} + \frac{1}{R_{th,mellor(or)}}} - \frac{T_o - T_b}{R_{th,7}} - \frac{T_o - T_l}{R_{th,or}} \\
N m_b c_p \frac{dT_b}{dt} &= \dot{Q}_b + \frac{T_o - T_b}{R_{th,7}} - \frac{T_b - T_i}{R_{th,8}} - \frac{T_b - T_l}{R_{th,b}} \\
m_i c_p \frac{dT_i}{dt} &= \dot{Q}_i + \frac{T_b - T_i}{R_{th,8}} - \frac{T_i - T_s}{\frac{1}{R_{th,13}} + \frac{1}{R_{th,mellor(ir)}}} - \frac{T_i - T_l}{R_{th,ir}} \\
m_s c_p \frac{dT_s}{dt} &= \frac{T_i - T_s}{\frac{1}{R_{th,13}} + \frac{1}{R_{th,mellor(ir)}}} - \frac{T_s}{\frac{1}{R_{th,mellor(is)}}}
\end{aligned}
\tag{14}
$$

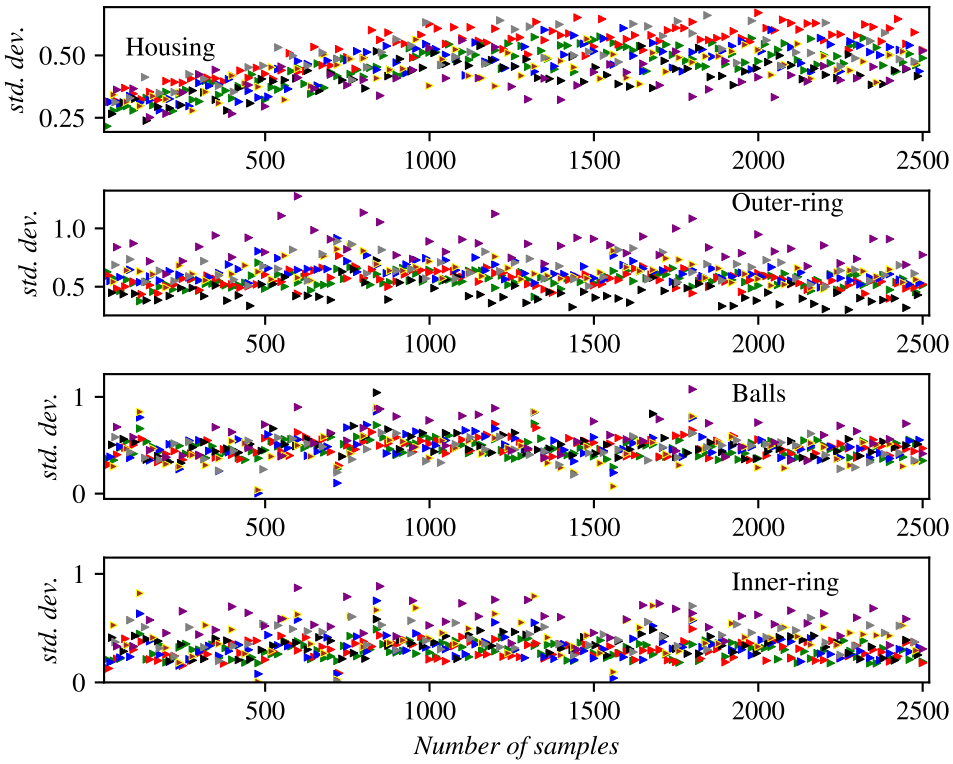

Figure 9: dispersion analysis for the components of the rolling bearing using the Light Gray-Box LPTN model.

I have introduced two thermal models, referred as the Light Gray-Box LPTN and White-Box LPTN. The light Gray-Box LPTN, comprises nine diffusion nodes. This thermal network incorporates the contact resistances of elliptical contact for stationary, moving, and combined heat sources, based on the investigation by Y. S. Muzychka et al. The White-Box LPTN is a more complex thermal model,

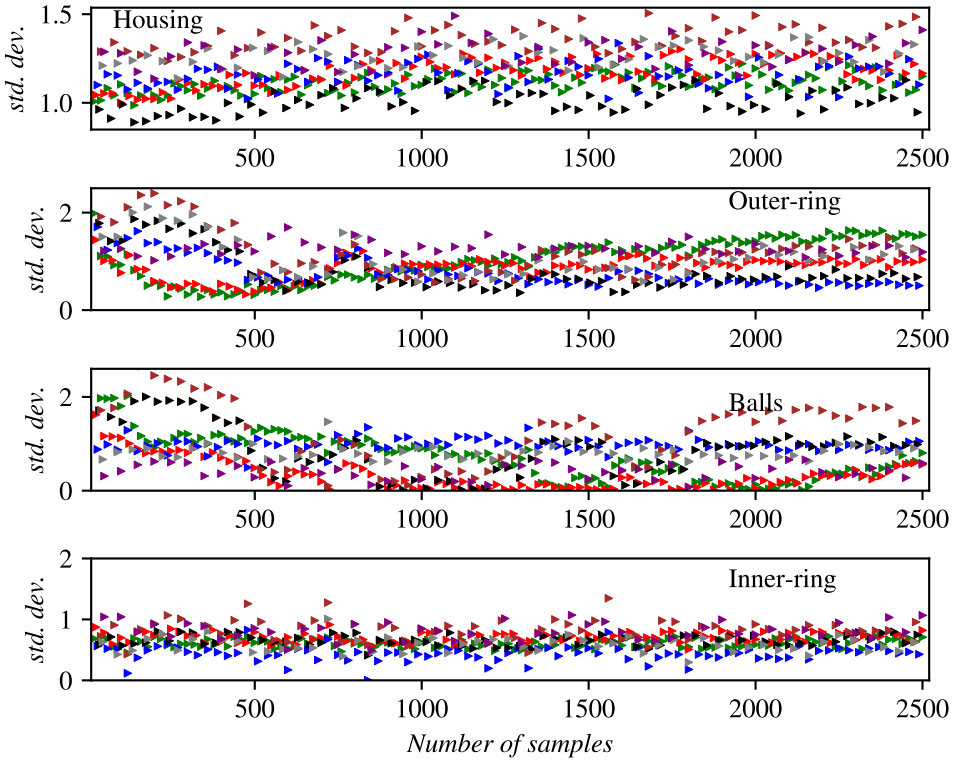

Figure 10: Dispersion analysis for the components of the rolling bearing using the White-Box LPTN model.

which comprises 17 diffusion nodes. This thermal Network utilizes the concept of contact resistances for moving and combined heat sources. Furthermore, the model incorporates the Mellor's formulation. Both models were solved for steady-state and continuous-time operations. Under steady-state conditions, the maximum percentage deviation was 2.2 % and 1.26 %, for the Light Gray-Box and White-Box LPTN, respectively. In continuous-time, the maximum dispersion was 2.97 for the Light Gray-Box LPTN, and 1.33 for the White-Box LPTN. Both thermal networks exhibit improved performance compared to the Dark Gray-Box LPTN. Among the models, the White-Box LPTN demponstrates the highest accuracy.

5 New scientific results and contributions

The following chapter presents the new contributions derived throughout this research process. The dissertation is divided into six chapters to facilitate readibility and comprehension for the reader, beginning from the introduction of the topic, followed by the research review. Subsequently, the description of the concepts and mathematical formulations necessary to implement in the thermal models are detailed. After this extensive process, the thermal models presented in Chapters Five and Six were developed. Based on the content of this document, the following theses are derived:

5.1 Theses

T1. I have modeled the thermal losses and the heat transfer of an angular contact ball bearing, specifically for spindle units. The heat transfer was based on the analysis of frictional moments resulting from the dynamic equivalent radial load. I separated the bearing elements housing, outer-ring, balls, and inner-ring into individual control volumes and applied the concept of heat partition for rolling and sliding elastohydrodynamic contacts [63]. This methodology enabled the treatment of the bearing elements as individual heat sources. I observed that the thermal losses and the heat transfer govern the steady conditions of the system. To solve the thermal system, I employed an analogy between electrical and thermal systems. Based on this analogy, I implemented the state-space approach, considering the thermal model of the bearing as a MIMO (multiple-input - multiple-output) system. The system showed the following features:
a) The thermal model was controllable and observable. However, for this research, the model's importance lies in its obsevability, as the thermal behavior can be predicted.
b) The State-space approach was applied to the thermal models: Dark Gray-Box, Light Gray-Box, and White-Box LPTN. I found that the steady state solutions closely match with the experimental and FEA simulations. For the Dark Gray-Box, and Light Gray-Box LPTN, the maximum percentage of dispersion was 3. 05 %. For the White-Box LPTN, the maximum percentage of dispersion was 1.26 %.
Related publications: [**P1**].

T2. I have implemented the formulations for thermal resistance models for non-circular moving heat sources [93]. I found that more accurate results are obtained when the contact between the elements of the angular contact ball bearing are realistic. Specifically, the contact between the outer-ring and the balls must be considered as a combined heat source, comprising both, stationary and moving heat

sources. For the contact between the balls ad the inner-ring, I found that the best approach is to treat the thermal contact as a moving heat source. When this considerations were implemented, the results improved drastically, closely matching with the experimental and FEA simulations with a dispersion of less than 1.04. Throughout this research, it was seen that, due to the small contact areas between the elements of the bearing (analyzed using the Hertzian contact theory), the models remain consistent and yield accurate results when assuming iso-flux distribution.
Related publications: [**P2**], [**P3**].

T3. I have created a new thermal model based on the global identification of Lumped parameter thermal networks, called Dark Gray-Box LPTN. I found that the model yields good thermal solutions if the conceptualizations of diffusion nodes and heat paths are clearly grounded in heat transfer theory. The model is efficient for both, steady and continuous-time solutions, considering that the number of nodes are no more than five. To improve the model's accuracy, I observed that implementing Walther's approach for the elastohydrodynamic lubrication, enhances the results by 5 %. The Dark Gray-Box LPTN model is designed to assist engineering of spindle systems in the early stage of development, without relying on complicated, costly, and time-consuming methods.
Related publications: [**P3**].

T4. I have created a thermal model called Light Gray-Box LPTN. The model consists of nine diffusion nodes. The nodes and heat paths implemented in the thermal network, allowed me to account for static thermal resistances for the housing, combined thermal contact resistances for the outer-ring and balls and moving heat sources for the balls and inner-ring. The thermal contact resistances were calculated for isoflux heat distribution. The heat transfer by convection was analyzed between the housing and the surroundings as a solid cylinder in air cross-flow at low speeds. I found that the discrepancy between the thermal model and the experimental and FEA simulations was less than 2.97 for continuous-time solutions. The model yields accurate results compared to experimental and FEA simulations.
Related publications: [**P2**], [**P4**], [**P5**] .

T5. I have created a thermal model called White-Box LPTN. The thermal network incorporates the concept of thermal resistances for static, moving, and combined heat sources, similar to the Light Gray-Box LPTN. Additionally, the thermal network incorporates the Mellor's formulation. I have found that through the application of the Mellor's formulation for cylindrical shapes (inner-ring, outer-ring and shaft), the axial and radial flow can be included in the mathematical formulation, enhancing the accuracy of the thermal model. Based on the statistical analysis, it is evident that the levels of discrepancy dicreased significantly. For the housing T_h, the maximum dispersion was 0.67. For the outer-ring T_o, was 1.33. For the balls T_b, the dispersion was 1.04, and for the inner-ring T_i, the maximum dispersion was 0.99. The model matches closely to the experimental and FEA results.
Related publications: [**P1**], [**P2**], [**P5**], [**P6**] .

6 Related publications

P1. Sebastian Cabezas, György Hegedűs, Péter Bencs, *"A New Thermal Model of an Angular Contact Ball Bearings, in a Standard Arrangement, subjected to Radial Loads, based on State Variables and Control Volumes",* Acta Polytechnica Hungarica, 2024, Vol. 21 (4).
Index: **Scopus**, Rank (**Q2**)

P2. Sebastian Cabezas, György Hegedűs, Péter Bencs, *"Thermal contact resistance for stationary and moving heat sources in angular contact ball bearings",* Tribology and Materials, 2023, Vol. 21 (3).
Index: **Scopus**.

P3. Sebastian Cabezas, György Hegedűs, Péter Bencs, *"Dark Gray Box Lumped Parameter Thermal Network for High Speed Spindle Rolling Bearings",* IEEE 21st Jubilee International Symposium on Intelligent Systems and Informatics, 2023.
Index:**Scopus**.

P4. Sebastian Cabezas, György Hegedűs, Péter Bencs, *"Transient heat convection analysis of a single rod in air cross-flow",* Pollack Periodica, 2023, Vol. 18 (2).
Index: **Scopus**, Rank (**Q3**)

P5. Sebastian Cabezas, Dániel Tóth, György Hegedűs, Péter Bencs,*"Thermal Model of a Ball Bearing using the State-Space approach and Light Gray-Box Lumped Parameter Thermal Network",* Power System Engineering 2023, 2023, Vol. 5 (383).

P6. Sebastian Cabezas, György Hegedűs, Péter Bencs, *"Thermal Experimental and Numerical Heat Transfer Analysis of a Solid Cylinder in Longitudinal Direction",* Analecta Technica Szegedinensia, 2023, Vol. 17 (1).

P7. Mohammad Alzghoul, Sebastian Cabezas, Attila Szilágyi*"Dynamic modeling of a simply supported beam with an overhang mass",* Pollack Periodica, 2022, Vol. 17 (2).
Index: **Scopus**, Rank (**Q3**)

P8. Sebastian Cabezas, Attila Szilágyi*"Thermal Behavior in Cnc Machine-Tools",* Design of Machines and Structures, 2020, Vol. 10 (2).

P9. Sebastian Cabezas, Attila Szilágyi*"Thermal and Structural Simulations of a Cnc Turning Center",* Design of Machines and Structures, 2020, Vol. 10 (2).